Preparation and Properties of Nanocomposite Hydrogels Containing Silver Nanoparticles by Ex Situ Polymerization

Wen-Fu Lee, Kai-Tai Tsao

Department of Chemical Engineering, Tatung University, Taipei, Taiwan, Republic of China

Received 26 August 2005; accepted 12 September 2005
DOI 10.1002/app.23171
Published online in Wiley InterScience (www.interscience.wiley.com).

ABSTRACT: A series of composite hydrogels containing silver nanoparticle used for bioadhesives were prepared from acrylic acid, poly(ethylene glycol) methyl ether acrylate, and silver nanoparticles through ex situ polymerization. Silver nanoparticles with a narrow size distribution were prepared by the reduction of a silver nitrate solution with ascorbic acid. The influence of the content of the silver nanoparticles in the hydrogels on the equilibrium swelling ratio, mechanical properties, electrical conductivity, and inactivation of *Escherichia coli* (*E. coli*) was investigated in this study. The results showed that the swelling ratios of the composite gels were reduced by silver nanoparticles in the gels but were not reduced with an increase in the content of silver nanoparticles. In addition, the crosslinking density and shear modulus of these hydrogels did not increase with an increase in the content of silver nanoparticles. The adhesive force of these hydrogels (the APECAg series) was not obviously changed. Finally, the initial rate of *E. coli* inactivation for the APECAg series hydrogels showed excellent antibacterial properties. © 2006 Wiley Periodicals, Inc. J Appl Polym Sci 100: 3653–3661, 2006

Key words: adhesives; hydrogels; nanoparticles

INTRODUCTION

Silver powders with ultrafine and uniformly distributed sizes have considerable current use. Silver is superior to other nanostructured metal particles with respect to electrical conductivity, bactericidal action, optical properties, and use in oxidative catalysis. In this respect, nanosized powders and colloidal dispersion of silver have attracted a great deal of attention in recent years.

Several methods used in the past to prepare silver nanoparticles, such as chemical reduction,[1–3] photochemical or radiation–chemical reduction,[4,5] microwave-assisted,[6] and sonochemical methods,[7] are being applied currently to prepare ultrafine silver powders. Using ascorbic acid as a reduction agent for silver nitrate ($AgNO_3$) was studied previously by Sondi et al.[8] Their results indicated that the experimental conditions, that is, the pH of the reacting solutions, the concentration of the stabilizing agent, and the metal/dispersant ratio, also have a significant impact on the size and stability of these dispersions. They showed an excellent ability to prevent the aggregation of nanosized silver at a high ionic strength and a high concentration of the metal.

Bioadhesive is defined as the adhesion of a polymer and a biological structure and is used for many hard- and soft-tissue applications. The term *bioadhesive* is applied when the substrate is mucus. Some researchers have made the conclusion that polymer characteristics are necessary for a bioadhesive, and they can be summarized as follows: strong hydrogen-bonding groups (—OH and —COOH), strong anionic charge (COO^- and SO^{3-}), high molecular weight, sufficient chain flexibility, and surface energy properties favoring the spread onto mucus.[9,10] In recent years, drug delivery systems using bioadhesive drug carriers have became increasingly important because of their ability to adhere to mucosal surfaces of the buccal and skin, thereby increasing therapeutic efficiency.[11,12] Typical polymers that have been used as mucoadhesive drug carriers include poly(acrylic acid) (PAA), poly(methacrylic acid), carboxymethylcellulose, and hydroxypropyl methylcellulose.[13,14] A wide range of polymers, both natural and synthetic, have been studied for their potential use as mucoadhesives.[15–19] Among the investigated polymers, PAA and its lightly crosslinked polymer have been shown to be good bioadhesives because of their hydrophilic nature, negative charge, and high flexibility.

Yasuo et al.[20] studied composite films consisting of metallic Cu nanoparticles dispersed in an acrylic acid (AA) gel. Cu nanoparticle/AA composite films were prepared by the reduction of Cu^{2+} from the copper salt of AA at a high temperature under H_2. Their results indicated that the color of the AA–Cu^{2+} films heated above 220°C changed from blue-green to deep red, and an optical absorption at about 570 nm was observed, caused by the surface plasma resonance

Correspondence to: W.-F. Lee (wflee@ttu.edu.tw).

TABLE I
Compositions and Swelling Ratio (Q) Values of the APECAg Series Hydrogels

Sample	APE0	APECAg1	APECAg1.5	APECAg2	APECAg2.5
AA (mol %)	90	90	90	90	90
PEGMEA (mol %)	10	10	10	10	10
EGDMA (mol %)	1	1	1	1	1
Ag (ppm)[a]	—	28.6	43	57.5	71.9
DEAP (mol %)	1	1	1	1	1
Ag conversion					
%	0	92	89	86	91
ppm	—	26.3	38	49.4	65.4
Yield (%)	91.8	94.2	90.5	92.3	89.1
Q (g/g)	1.64	0.97	0.96	0.94	0.93

[a] Based on the total monomer weight.

absorption of Cu nanoparticles. Cu nanoparticles dispersed homogeneously in the films, and the diameters were in the range of 10–16 nm. Some polymers containing silver nanoparticles were reported by Zhang and coworkers.[6,21] They reported the characteristic and reduction mechanism of polyacrylonitrile containing silver nanoparticles. Their results showed that silver nanoparticles with narrow size distributions were obtained and were well dispersed in the polyacrylonitrile matrix.

In this study, silver nanoparticles were prepared through the reduction of a $AgNO_3$ solution by ascorbic acid in advance. Then, the silver nanoparticle solution was incorporated into an AA and poly(ethylene glycol) methyl ether acrylate (PEGMEA) solution to perform ex situ photopolymerization. The various properties of the obtained composite hydrogels were investigated.

EXPERIMENTAL

Materials

AA and diethoxyacetophenone (DEAP) as a photoinitiator were purchased from Fluka Chemical Co (Buchs, Switzerland). PEGMEA (number-average molecular weight = 454) and L-ascorbic acid were purchased from Aldrich Co. and Sigma Co (St. Louis, MO), respectively. $AgNO_3$, purchased from Nihon Shiyaku Industries, Ltd. (Osaka, Japan), and ethylene glycol dimethacrylate (EGDMA) as a crosslinker, purchased from TCI (Tokyo, Japan), were used as received. *Escherichia coli* (*E. coli*) ATCC 8739 was purchased from the Food Industry Research and Development Institute (Taipei, Taiwan). Luria bertani (LB) medium and agar powder were purchased from Difco (Franklin Lakes, NJ). All solvents and other chemicals were used as received, except for AA, which was purified by vacuum distillation at 29°C and 6 mmHg.

Preparation of the silver nanoparticles and composite hydrogels

To prepare silver nanoparticles, 100 mL of a 100 ppm ascorbic acid solution was added to 100 mL of 100 ppm aqueous $AgNO_3$ at room temperature. The silver nanoparticles formed rapidly after these solutions were mixed. An appropriate amount of the silver nanoparticle solution listed in Table I was incorporated into an AA and PEGMEA monomer solution, with a fixed molar ratio (9/1), and then 1 mol % EGDMA as a crosslinker and 1 mol % DEAP as a photoinitiator were added. The mixture was then injected into the space between two glass plates with 2-mm silicone rubber as a spacer. Polymerization was carried out via the exposure of the monomer solution to UV irradiation (full-length, 600 W) for 8 min. After gelation was completed, the gel membrane was cut into disks, 10 mm in diameter, and immersed in an excess amount of deionized water for 3 days to remove residual components. The sample codes, yields, and equilibrium swelling ratios of the nanocomposite gels are listed in Table I.

Measurement of the conversion of aqueous $AgNO_3$ into solid Ag

The feed compositions of the composite polymers were similar to those for the preparation of the composite hydrogels, as previously mentioned, except that the crosslinker was not added. The polymerization was carried out via the exposure of the monomer solution to UV irradiation for 8 min. To dissolve the gel, the obtained gel was heated to 100°C in 100 mL of a water solution for 48 h. Finally, the 10-mL residual solution was examined with atomic absorption spectrometry (AAS; model 3000, Varian, Osaka, Japan). The calibration curve of silver was prepared in advance, as shown in Figure 1.

Measurement of the equilibrium swelling ratio

The preweighed dried gels (W_d) were immersed in deionized water at 25°C until the swelling equilibrium was attained. Each gel was removed from the water bath, tapped with delicate task wipers to remove excess surface water, and weighed as the wet weight of

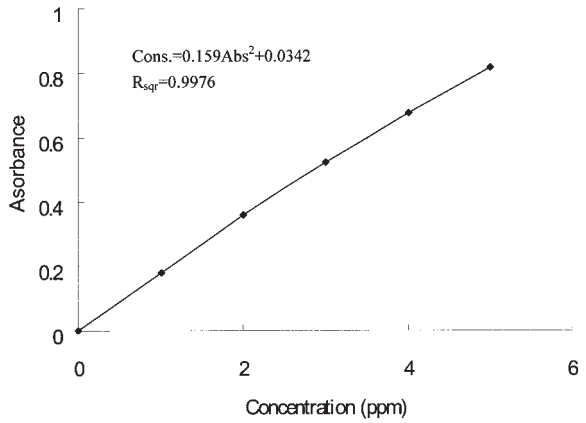

Figure 1 Calibration curve of the silver-ion concentration in AAS analysis.

the gel (W_w). The swelling ratio (Q) was calculated with the following equation:

$$Q = (W_w - W_d)/W_d \tag{1}$$

Swelling kinetics measurement

The swelling ratio was obtained through the weighing of the initial and swollen samples at various time intervals. The amount of water absorbed (W_t) was reported as a function of time, and the equilibrium absorption at an infinitely long time was designated W_∞. The following equation was used to calculate the diffusion coefficient (D) for $W_t/W_\infty \leqq 0.8$:[22]

$$W_t/W_\infty = (4/\pi^{0.5})(Dt/L^2)^{0.5} \tag{2}$$

where t is the time and L is the initial thickness of the dried gel. To investigate the diffusion model of the gel, the initial swelling data were fitted to the exponential heuristic equation for $W_t/W_\infty \leqq 0.6$:[23,24]

$$W_t/W_\infty = kt^n \tag{3}$$

where k is a characteristic constant of the gel and n is a characteristic exponent of the mode transport of the penetrate. In addition, the penetration velocity (ν) of water in each gel, which was described by Peppas and coworkers,[25,26] was determined as follows:

$$\nu = \frac{1}{2\rho_w A}\frac{dw}{dt} \tag{4}$$

where dw/dt is the slope of the curve of the weight gain versus time, ρ_w is the density of water, A is the area of one face of the disk, and factor 2 accounts for the fact that penetration takes place through both sides of the disk.

Physical property measurements

The gel strengths of these samples were measured with a uniaxial compression experiment with a universal tester (Lloyd LRX, J. J. Lloyd, Poole, UK). Equation (5) was used to calculate the shear modulus (G):[27,28]

$$\tau = F/A = G(\lambda - \lambda^{-2}) \tag{5}$$

where τ is the compression stress, F is the compression load, A is the cross-sectional area of the swollen gels, λ is the compression strain (L/L_0), L is the thickness of the wet gel after compression, and L_0 is the thickness of the dried gels. At low strains, a plot of τ versus $-(\lambda - \lambda^{-2})$ yields a straight line whose slope is G. The effective crosslink density (ρ_x) can be calculated from G and the polymer volume fraction (ν_2) as follows:

$$\rho_x = G/\nu_2^{1/3}RT \tag{6}$$

where R is the ideal gas constant and T is the absolute temperature.

Assessment of the adhesive force

The force detection system consisted of a precision load cell and roller with a universal tester (Lloyd LRX). The nanocomposite gels were cut into dimensions of 3 cm × 1 cm (thickness = 2.0 mm). Then, they were brought into contact with a poly(ethylene terephthalate) (PET) film on the roller. The peel strength was determined with a constant speed of 30 mm/cm, and the force required to fracture the adhesive bond was recorded.

X-ray diffraction (XRD) analysis

Powder XRD analyses were performed with a MAC Science X-ray powder diffractometer, with a Cu anode (model M21X, MAC Science, Osaka, Japan), running at 40 kV and 30 mA and scanning from 10 to 80° at 3°/min. Ag particles and dry APECAg hydrogels were tiled on the cell to examine XRD.

Measurement of the electrical conductivity

A Napson four-point probe measurement was used for the surface resistance study. The dry and wet hydrogels were cut into dimension of 2 cm × 2 cm (thickness = 2.0 mm). Equations (7) and (8) were used to obtain the surface resistance (R_s):[29,30]

$$R_s\left(\frac{\Omega}{sq}\right) = \frac{\pi}{\ln 2} \times \frac{V}{I} = 4.532 \times \frac{V}{I} \tag{7}$$

$$R_s \times d = \rho \tag{8}$$

where d is the thickness and ρ is the resistivity.

Bacterial culture

LB agar was composed of an LB medium and 15 g/L agar. A saline solution was autoclaved at 121°C for 15 min for sterilization. *E. coli* ATCC 8739 was maintained on an LB agar slant. One loop of bacterial cells was inoculated to 100 mL of the LB medium in a 500-mL Erlenmeyer flask. This was then cultured at 37°C and at a shaking speed of 170 rpm for 12–16 h. The resultant culture was used for the following experiment.

Assay of the antibacterial activity

One gram of a hydrogel was broken into fragments and then put into 500-mL Erlenmeyer flasks containing 100 mL of sterile water. After the addition of 1.0 mL of the bacterial culture, as previously mentioned, the flasks were incubated in a 37°C shaker, and samples were taken at 20, 40, 60, and 120 min. The samples were stepwise diluted 10^3- and 10^5-fold with 0.85% saline solutions. Then, the molten LB agar, sterilized, was cooled in a 50°C water bath and poured into Petri dishes (ca. 15 m per Petri dish) containing 1.0 or 0.1 mL of the diluted samples. After thorough mixing of the bacterial dilutions and agar media by gentle shaking, the agar media were left to stand for solidification. Colonies that developed on the agar plates after incubation at 37°C for 2 days were counted. The viabilities were determined by the pour plate method. The inactivation of *E. coli* was evaluated by a comparison of the changes in viability during the incubation in the shaken flask culture. The viability was presented as log cfu/mL.

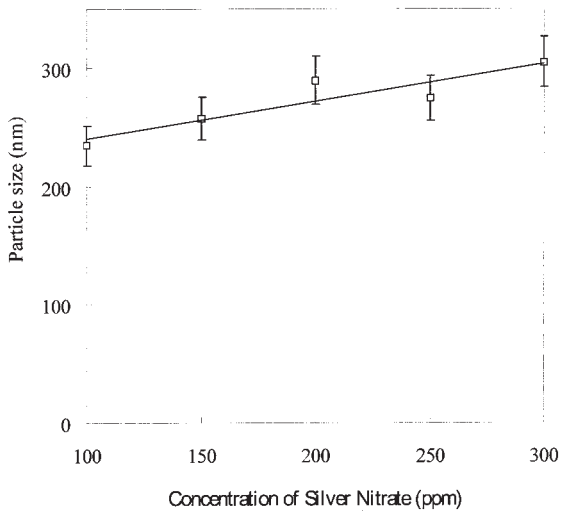

Figure 2 Effect of the concentration of $AgNO_3$ on the particle size of silver particles reduced by ascorbic acid under pH 6.7.

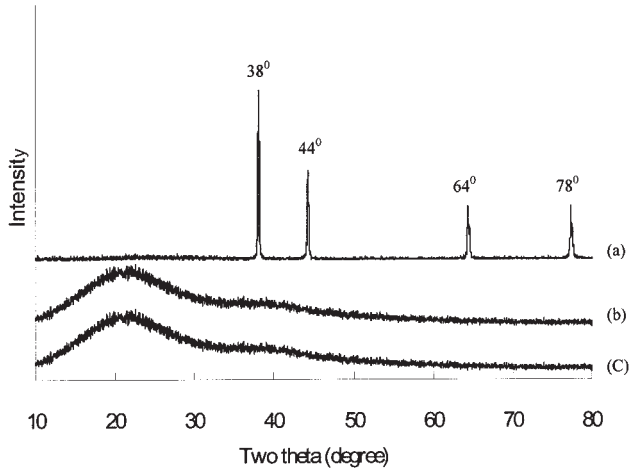

Figure 3 XRD patterns of (a) the Ag particle and (b) the APECAg gel.

Morphology

The dry specimens were examined for morphological details with scanning electron microscopy (SEM; JSM-5300, JEOL, Tokyo, Japan) with an acceleration voltage of 15 kV. The specimens were coated with a gold metal layer to provide proper surface conduction.

RESULTS AND DISCUSSION

Synthesis of the silver nanoparticles

The silver nanoparticles were prepared by the reduction of aqueous $AgNO_3$ into solid Ag with ascorbic acid. The effect of the concentration of $AgNO_3$ on the silver particle size is shown in Figure 2. The results shown in Figure 2 indicate that the silver particle size approximately linearly increased with the concentration of the $AgNO_3$ solution from 230 to 300 nm at pH 6.7. This occurred because the silver nanoparticles

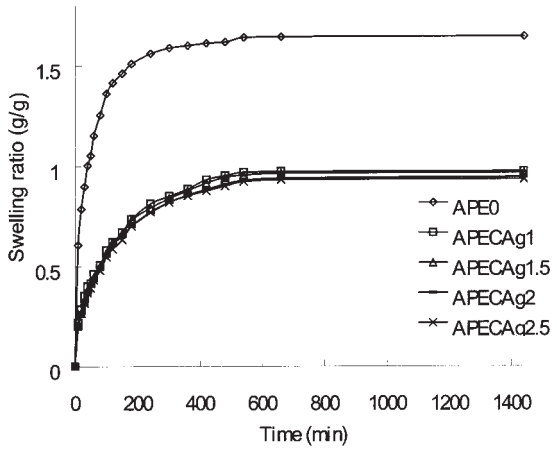

Figure 4 Swelling ratio as a function of time for an APECAg hydrogel in deionized water at 25°C.

TABLE II
Diffusion Coefficient (D) and Penetration Velocity (ν) Values for the Composite Hydrogels

Sample	$D \times 10^8$ (cm/s^2)	ν (cm/min)
APE0	7.05	0.329
APECAg1	7.01	0.164
APECAg1.5	6.22	0.154
APECAg2	6.08	0.148
APECAg2.5	5.94	0.13

TABLE IV
Electrical Conductivity (R) of the APE0 and APECAg Series Hydrogels

Sample	Dry hydrogel R (Ω cm)	Wet hydrogel R (Ω cm)
APE0	$3.0 \times 10^{10} \pm 1.2 \times 10^9$	$24872.5 \pm 3.8 \times 10^3$
APECAg1	$2.8 \times 10^8 \pm 9.2 \times 10^6$	9835.3 ± 731
APECAg1.5	$2.7 \times 10^8 \pm 1.4 \times 10^6$	8482.1 ± 315
APECAg2	$2.7 \times 10^8 \pm 9.8 \times 10^6$	8319.8 ± 507
APECAg2.5	$2.5 \times 10^8 \pm 1.3 \times 10^6$	7536 ± 678

readily aggregated when the concentration of the $AgNO_3$ solution was increased. The conversion of the silver ions reduced into silver particles was up to 89% under weak acid conditions, as shown in Table I.

Identification of the silver nanoparticles

The XRD patterns of various samples are plotted in Figure 3. The XRD pattern of the AA/PEGMEA copolymeric gel shows a sharp crystalline peak at 22° [Fig. 3(c)]. The XRD patterns of the silver powder and the APECAg2.5 gel are shown in Figure 3(a,b), respectively. The silver particles show diffraction peaks with 2θvalues of 38, 44, 64, and 78°, corresponding to crystal planes of (111), (200), and (220) of face-centered cubic crystalline silver [see Figure 3(a)], and a lattice parameter of 0.4089 nm. This conforms to the reported data (JCPDS File No. 4-0783).[6] However, the APECAg2.5 gel does not show any diffraction peak in the XRD pattern. This may be attributed to the fact that the silver particles were embedded in the gel.

Effect of the silver nanoparticle content on the swelling kinetics

The swelling ratios as a function of time for these composite hydrogels in water solutions at 25°C are shown in Figure 4. The results show that the equilibrium swelling ratio decreased when the silver nanoparticles were incorporated into the gels (also see Table I), but the equilibrium swelling ratios of the composite gels were not affected by the added contents of silver nanoparticles. This behavior can be presumed from the fact that the surface pores of the composite gels were blocked with silver particles. This blocking effect, shown in Figure 4, was not significant with increasing silver particle content.

The diffusion coefficient of water diffusing into the composite gels and the penetration velocity of water into the gels could be calculated with eqs. (2) and (4), respectively.

The results in Table II indicate that both the diffusion coefficient and penetration velocity showed a tendency to decrease when the content of silver nanoparticles increased. This was because the pores inside the composite hydrogels were easily blocked by silver nanoparticles, and this resulted in the difficulty of water penetration into the interior of the gels.

Effect of the silver nanoparticle content on the gel strength and crosslinking density

The gel strength was accessed by the shear modulus obtained from eq. (5). The results in Table III show that the gel strength of the nanocomposite hydrogels increased with an increase in the silver nanoparticle contents (from 218.63 to 252.3 g/cm^2). The effective crosslinking density is defined as the concentration of elastically active chains (chains are deformed by an applied active stress) in the polymer network and is usually reported on the basis of moles of chains per

TABLE III
Physical Properties of the APECAg Series Hydrogels

Sample	Effective crosslink density $\rho \times 10^5$ for the wet gel (mol/cm^3)	Sheer modulus (g/cm^2)	Adhesive force (g/cm^2)
APE0	1.74 ± 0.03	218.63 ± 21	$16.73 \pm 0.3\%$
APECAg1	1.75 ± 0.03	232.32 ± 18	$15.61 \pm 0.8\%$
APECAg1.5	1.81 ± 0.06	239.64 ± 31	$15.3 \pm 1.1\%$
APECAg2	1.82 ± 0.02	242.71 ± 14	$16.53 \pm 0.8\%$
APECAg2.5	1.85 ± 0.07	252.33 ± 29	$15.81 \pm 0.6\%$

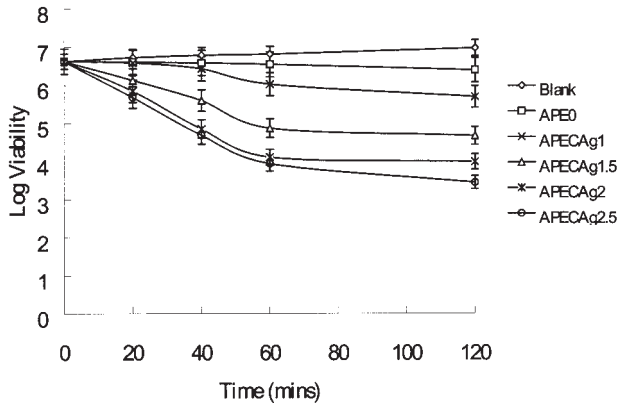

Figure 5 Inactivation of *E. coli* for the APECAg series hydrogels as a function of time.

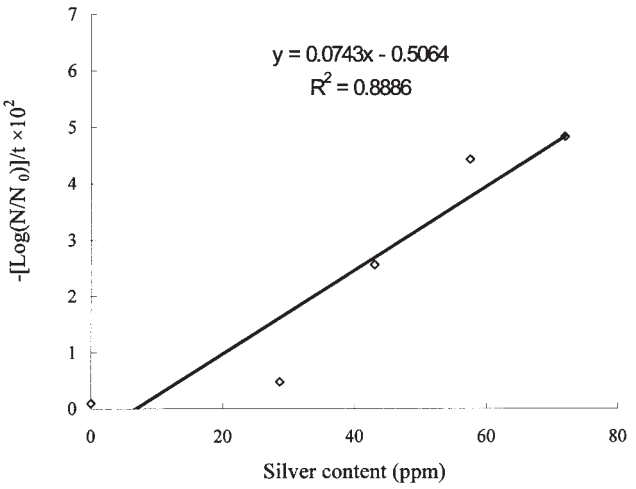

Figure 6 Initial rate of bacterial inactivation $\{-[\log(N/N_0)]/t \times 10^2\}$ as a function of the silver content in the APECAg series hydrogels.

cubic centimeter of dry polymer. The effective crosslinking densities for the composite hydrogels were obtained with eq. (6). The results shown in Table II indicate that the effective crosslinking densities were only slighted enhanced by an increase in the silver nanoparticle contents in the hydrogels. These results explicitly indicate that the silver nanoparticles were uniformly dispersed in the composite hydrogels but did not participate in the crosslinking reaction with the polymer matrices.

Effect of the silver nanoparticle contents on the adhesive force

The adhesive forces of the nanocomposite hydrogels are also shown in Table III. The adhesive force was determined by the measurement of the force required to break the adhesive surface between the substrate (PET film) and the gels. The results in Table III show that the APECAg series hydrogels were not significantly changed with an increase in the silver nanoparticle content. This was because that the silver particles did not hamper the AA functional group on the surface.

Effect of the silver nanoparticle content on the electrical conductivity

The effect of the silver nanoparticle content on the electrical conductivity of the composite hydrogels is shown in Table IV. The results in Table IV show that the electrical resistance of the gels decreased 2 orders when the silver nanoparticles were incorporated into the APE0 gel for dry-state gels. However, for wet-state gels, the resistance decreased from 10 orders of the dry gel to 5 orders of the wet gel for the APE0 gel. This phenomenon shows that water provides a path for the electric current in the gel. However, when the silver nanoparticles were incorporated into the gels, the resistance decreased with an increase in the silver content of the gels. This occurrence showed that the silver particle in the gels actually could improve the electri-

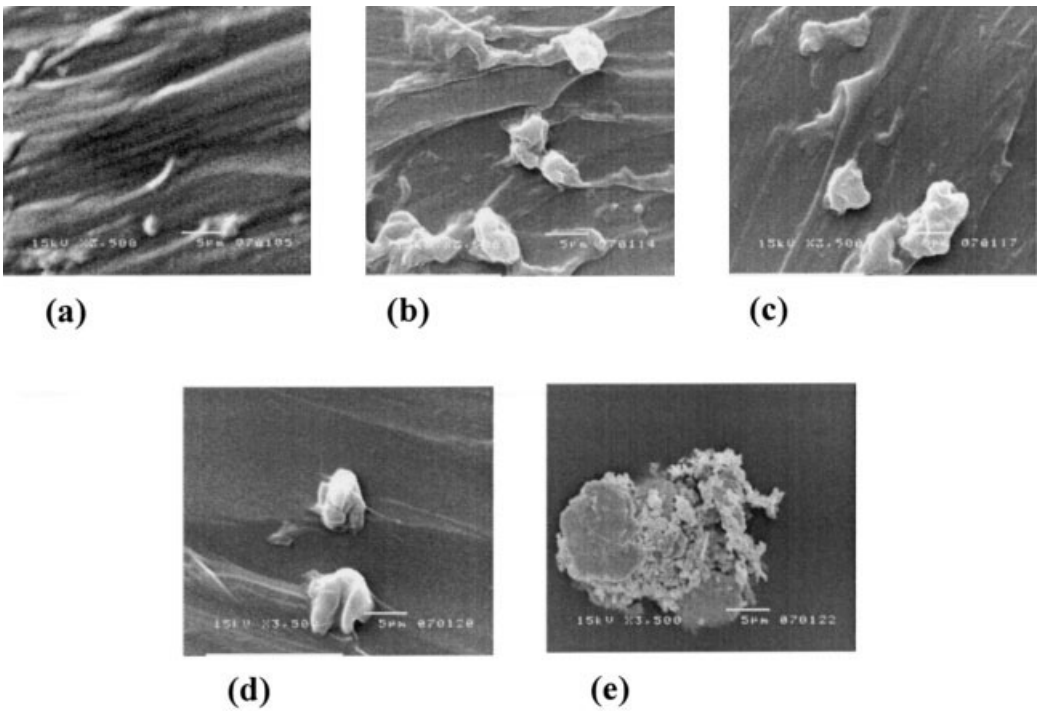

Figure 7 Cross-sectional microphotographs for APECAg hydrogels: (a) APE0, (b) APECAg1, (c) APECAg1.5, (d) APECAg2, and (e) APECAg2.5 (3500×).

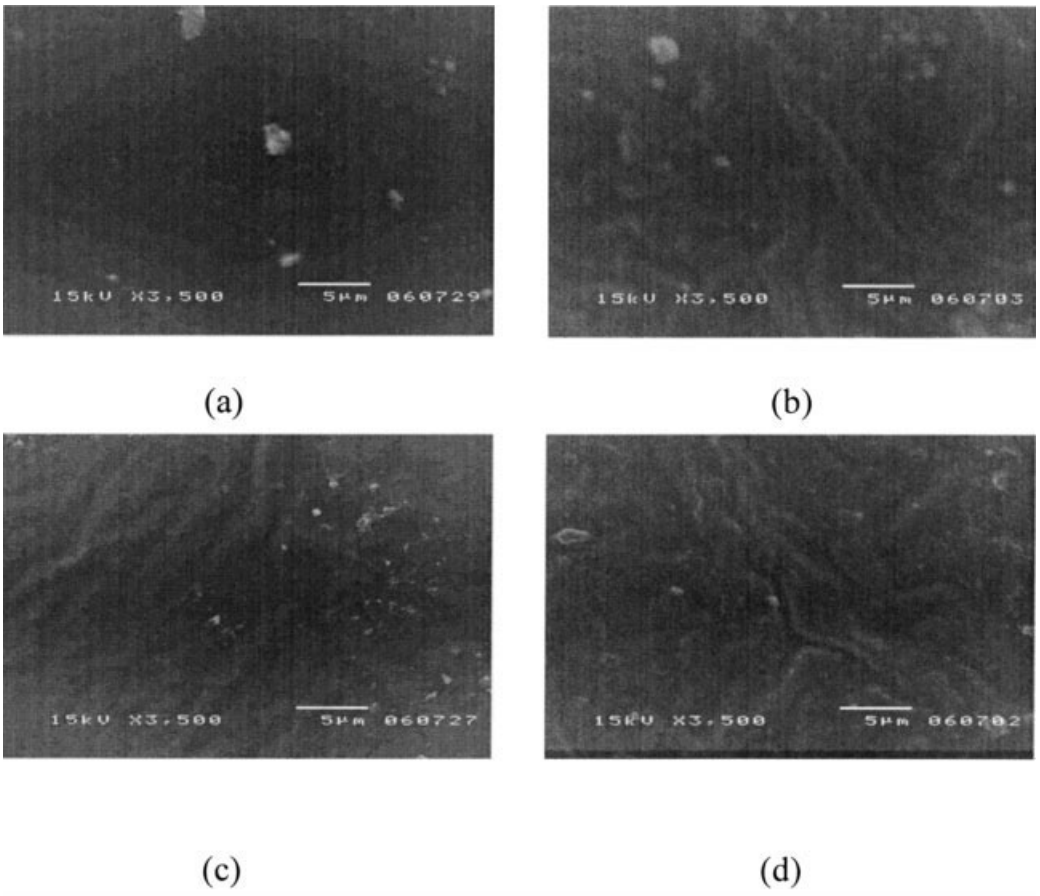

Figure 8 Surface microphotographs for APECAg hydrogels: (a) APECAg1, (b) APECAg1.5, (c) APECAg2, and (d) APECAg2.5 (3500×).

cal conductivity of the composite gels. This behavior could lead to composite gels being used in electrostimulus bioadhesive patches.

Effect of the silver nanoparticle content on *E. coli* inactivation

It is well known that silver nanoparticles have a bacterial inactivation effect and inflammation action. The inactivation of *E. coli* for the APECAg series gels as a function of time is shown in Figure 5. The results shown in Figure 5 indicate that the tendency of bacterial inactivation for the APE series gels was in the order APECAg2.5 > APECAg2.0 > APECAg1.5 > APECAg1.0 > APE0. That is, the bacterial inactivation of the APECAg series gels increased with an increase in the silver content in the composite gels.

Effect of the silver nanoparticle content on the first-order destruction of *E. coli*

The effect of the silver nanoparticle content on the first-order destruction of the bacteria was evaluated. The expression of the first-order response mathematically can be given as follows:

$$\frac{-dN}{dt} = kN \tag{9}$$

where $-dN/dt$ is the rate at which the concentration decreases, N is the concentration of viable microorganisms, and k is the rate constant of a first-order reaction. The initial rate of bacterial inactivation as a function of the silver content in APECAg gels is shown Figure 6. The results in Figure 6 indicate that the inactivity effect was an approximately linear relation within the silver content range of 28.6–71.9 ppm.

SEM

Cross-sectional and surface microphotographs for APECAg series nanocomposite hydrogels are shown in Figures 7 and 8, respectively. The surface and cross-sectional faces are very smooth; the silver particles were not obviously observed with SEM.

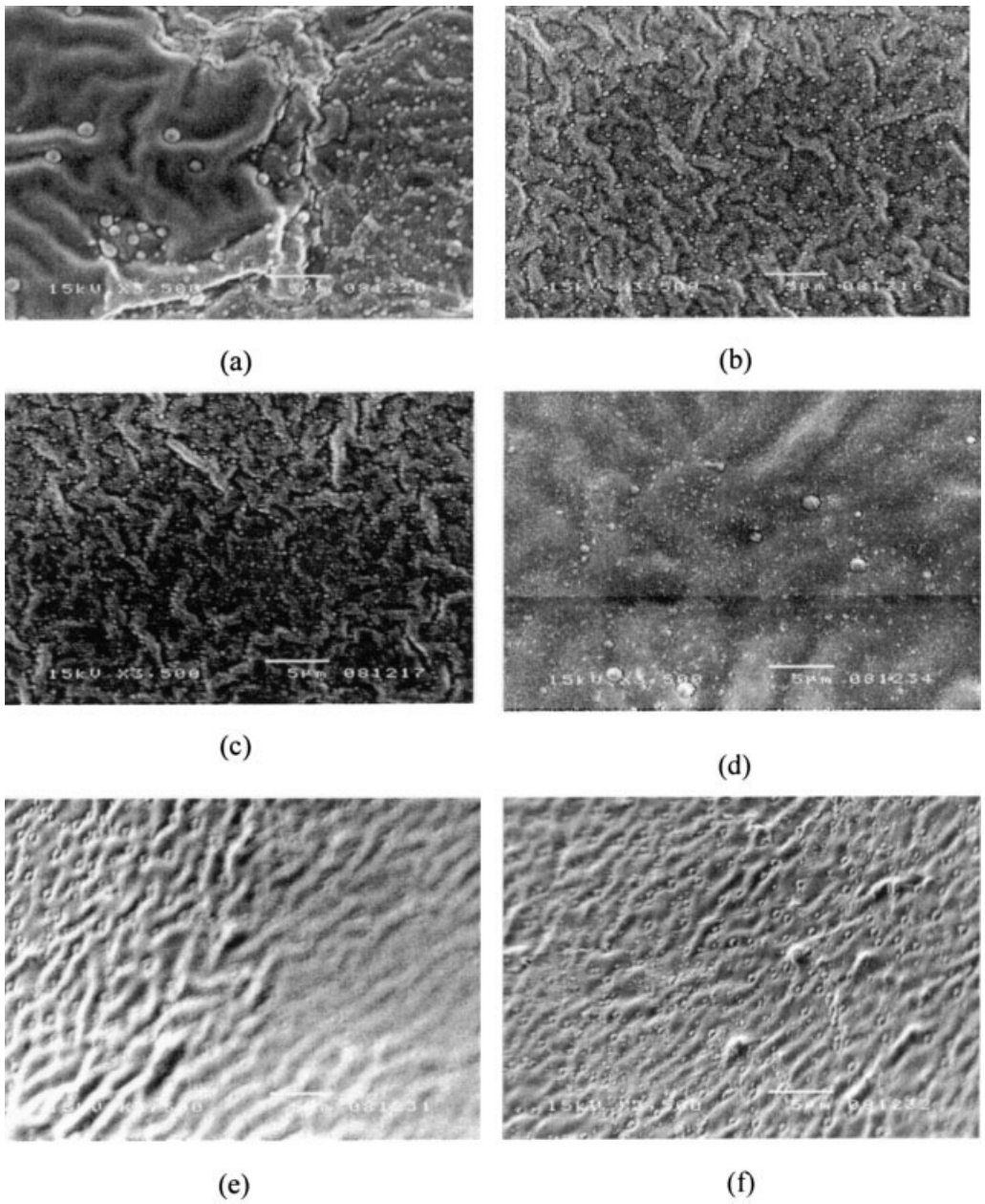

Figure 9 SEM microphotographs for APECAg hydrogels at the surface (S) and cross section (V): (a) APECAg1.0-S-6 h, (b) APECAg1.0-S-24 h, (c) APECAg1.0-V-6 h, (d) APECAg2.0-S-6 h, (e) APECAg2.0-S-24 h, and (f) APECAg2.0-V-6 h.

That is, the silver particles were embedded inside the gels. To confirm this, typical gels were treated with 6*N* HNO_3 for 6 and 24 h at room temperature. The SEM images of the treated gels in Figure 9 show the silver particles more significantly than Figure 9(a,b). In addition, the silver particles appearing in the cross-sectional face are more numerous than those appearing at the surface. From these results, we can confirm that the silver nanoparticles were embedded inside the gels. This behavior proved that the swelling ratio and penetration velocity decreased with the silver content in the gels.

CONCLUSIONS

Poly[acrylic acid-*co*-poly(ethylene glycol) methyl ether acrylate]/silver nanoparticle composite hydrogels were successfully synthesized by *ex situ* polymerization at room temperature. Some conclusions can be made from the discussion as follows: the equilibrium swelling ratio decreased when the silver nanoparticles were incorporated into the gels, but the equilibrium swelling ratios of the composite gels were not affected by the added contents of silver nanoparticles. Both the diffusion coefficient and penetration velocity showed

a tendency of decreasing when the content of the silver nanoparticles increased. The gel strength of the nanocomposite hydrogels increased with an increase in the silver nanoparticle contents. In addition, the APECAg series hydrogels showed good electrical conductivity and *E. coli* inactivation. Finally, the silver nanoparticle position and silver nanoparticle size in hydrogels used for bioadhesive and electroactive gels will be studied in the future to improve the electrical conductivity.

The authors wish to thank the National Science Council of the Republic of China for financial support under Grant NSC 93-2216-036-01. The authors also thank Professor Dey-Chyi Sheu, for his excellent and skillful assistance in bacterial inactivation.

References

1. Okamoto, M.; Morita, S.; Taguchi, H.; Kim, Y. H.; Kotaka, T.; Tateyama, H. Polymer 2000, 41, 3887.
2. Ramos, J.; Millan, A.; Palacio, F. Polymer 2000, 41, 8461.
3. Zhu, Z. K.; Yin, J.; Cao, F.; Shang, X. Y., Lu, Q. H. Adv Mater 2000, 12, 1055.
4. Nersisyan, H. H.; Lee, J. H.; Son, H. T.; Won, C. W.; Maeng, D. Y. Mater Res Bull 2003, 38, 949.
5. Chou, K. S.; Ren, C. Y. Mater Chem Phys 2000, 64, 241.
6. Zhang, Z.; Zhang, L.; Wang, S.; Chen, W.; Lei, Y. Polymer 2001, 42, 8315.
7. Yener, D. O.; Sindel, J.; Randall, C. A.; Adair, J. H. Langmuir 2002, 18, 8692.
8. Sondi, I.; Goia, D. V.; Matijevic, E. J Colloid Interface Sci 2003, 260, 75.
9. Mortazavi, S. A. Int J Pharm 1995, 124, 173.
10. Chickering, D. E.; Mathiowitz, E. J Controlled Release 1995, 34, 251.
11. Florence, A. T.; Jani, P. U. Drug Saf 1994, 10, 233.
12. Hwang, S. J.; Park, H.; Park, K. Crit Rev Ther Drug Carrier Syst 1998, 15, 243.
13. Ahuja, A.; Khas, R. K.; Ali, J. Drug Dev Ind Pharm 1997, 23, 489.
14. Yang, X. J.; Robinson, R. In Biorelated Polymers and Gels: Controlled Release Application in Biomedical Engineering; Okano, T., Ed.; Academic: London, 1998; p 135.
15. Gandhi, R. E.; Robinson, J. R. Int J Pharm Sci 1988, 50, 145.
16. Chang, H. S.; Park, H.; Kelly, P.; Robinson, J. R. J Pharm Sci 1985, 74, 399.
17. Kriaet, B.; Kissel, T. Int J Pharm 1996, 127, 135.
18. Leung, S. S.; Robinson, J. R. J Controlled Release 1990, 12, 187.
19. Lether, C. M.; Bouwstra, J. A.; Schacht, E. H.; Junginger, H. E. Int J Pharm 1993, 78, 43.
20. Yasuo, G.; Ryo, I.; Yutaka, O.; Masanobu, N.; Kensuke, A.; Shigehito, D. J Mater Chem 2000, 10, 2548.
21. Liu, H.; Ge, X.; Ni, Y.; Ye, Q.; Zhang, Z. Rad Phys Chem 2001, 61, 89.
22. Kabra, B. G.; Gehnke, S. W.; Hwang, S. T. J Appl Polym Sci 1991, 42, 2409.
23. Franson, N. M.; Peppas, N. A. J Appl Polym Sci 1983, 28, 1299.
24. Korsmeyer, R. W.; Merrwall, E. W.; Peppas, N. A. J Polym Sci Part B: Polym Phys 1986, 24, 109.
25. Peppas, N. A.; Franson, N. M. J Controlled Release 1983, 21, 983.
26. Davidson, C. W.; Peppas, N. A. J Controlled Release 1986, 3, 259.
27. Peppas, N. A.; Barr-Howell, B. D. Hydrogels in Medicine and Pharmacy; CRC: Boca Raton, FL, 1986; Chapter 1, p 27.
28. Treloar, L. R. G. The Physics of Rubber Elasticity; Clarendon: Oxford, 1975.
29. Valdes, L. G. Proc IRE 1954, 42, 420.
30. Smits, F. M. BSTJ 1958, 37, 711.